Global Journal of Engineering and Technology [GJET].
ISSN: **2583-3359** (Online)
Frequency: Monthly
Published By GSAR Publishers
Journal Homepage Link- https://gsarpublishers.com/journal-gjet-home/

Finger Vein Segmentation in Infrared Images Based on Model Fitting

BY

M. VLACHOS[1] AND E. DERMATAS[2]

[1]Institute of Communication and Computer Systems, Athens, Greece
[2]Department of Computer Engineering and Informatics University of Patras, Patras, Greece

Article History

Received: 10/11/2023
Accepted: 09/01/2024
Published: 22/01/2024

Vol – 3 Issue – 1

PP: - 01-07

Abstract:

In this paper, a novel method for finger vein segmentation in infrared images based on a model that represents the intensity distribution along a cross-sectional profile of vein, is proposed. The method is based on model fitting of brightness intensities over a local neighborhood. A simple second-order degree polynomial is used in order to represent the brightness intensities along the cross-sectional profile of veins. Two different approaches are adopted. According to the first, a multiscale multidirectional model fitting is performed based on the assumption that the second-order derivative on a vein pixel is positive. The second is based on multiscale model fitting of intensities in a single direction using two assumptions about the intensities of the profile of veins. According to the first assumption, the second-order derivative is positive on a vein pixel and according to the second, the first-order derivative is zero on a vein pixel which means that the pixel belongs to vein centerlines. The proposed method is robust, in both approaches, as the experimental results show and it achieves high evaluation rates in terms of sensitivity, specificity, and accuracy.

1. Introduction

The problem of finger vein extraction arises mainly for biometrics purposes but it is also very important for the biomedical research community. Personal identification, which is the main application target in biometrics, can be applied to a wide range of applications including area access control, *PC* login, and e-commerce. Biometric systems like fingerprint, face, iris, retina, voice, and hand geometry recognition do not ensure necessarily confidentially because the estimated features can be recorded and reproduced by other means and suffer from several important weaknesses such as theft, loss, and reliance on the user's memory met in conventional methods such as keys, passwords, and *PIN* numbers. A biometric system which uses vein patterns overcomes these problems because the information used for identification include human biological attributes which are memory less, inside the human body.

Vein or vessel extraction is also very useful in several biomedical imaging applications, i.e. for diagnosing in vascular pathology. The inspection of angiogenesis in the human body can be used for early diagnosis of several diseases, both in healthy tissue for healing wounds and for restoring blood flow to tissues after injury or insult. Also, inspection of the retinal vasculature may reveal hypertension, diabetes, arteriosclerosis, cardiovascular disease, and stroke. Early detection of glaucoma, the second commonest cause of blindness in the West and the commonest cause of blindness worldwide, can be detected by inspection of the retinal vasculature.

The problem of finger vein pattern extraction from infrared images mainly involves the segmentation of the acquired images in two regions: vein and tissue. In these images, the veins appear darker than the surrounding tissue, due to strong absorption of light from the hemoglobin molecules, and they have a concave shape cross-sectional profile. This property can be used to facilitate the segmentation process and several researchers use the concave shape of the vein to achieve better segmentation results [6-7, 8, 14]. Primitive segmentation methods based on simple global thresholding techniques proved inadequate due to the fact that other parts of the finger have similar brightness and the image histogram is not bimodal. Moreover, infrared images suffer from several shading artifacts produced mainly due to uneven illumination, poor acquisition conditions, and fingerprint noise. Thus, brightness normalization and shading correction are popular preprocessing modules in such applications.

An application-specific vein pattern extraction method and a biometric identification system are presented in [1]. Typically, the vein pattern recognition algorithm consists of an original image-grabbing process, image preprocessing, and recognition. The preprocessing part consists of an iterative Gaussian low pass filter, a high pass filter, and a modified median filter [4]. In [1, 2, 4] low-pass spatial filtering for

*Corresponding Author: M. VLACHOS

noise removal and high pass spatial filtering for enhancing vascular patterns are used for vascular segmentation.

An improved vein pattern extraction algorithm is proposed in [3], which compensates the loss of vein patterns in the edge area, giving better image enhancement, improved vein pattern information, and better performance than the rate reported in [1]. The problem arising from the iterative nature of filtering preprocessing is solved by designing a filter that is used only once, significantly improving the recognition speed and simplifying the hardware complexity, using a Field Programmable Gate Array device (*FPGA*). The Fa1se Acceptance Rate (*FAR*) is five times better than the existing algorithm and the recognition speed is measured to be 100 ms/person.

In [5], a direction-based vascular pattern extraction algorithm based on the spatial information of vascular patterns is presented for biometric applications. It applies two different filters: row vascular pattern extraction filter for abscissa vascular pattern extraction, and column vascular pattern extraction filter for effective extraction of the ordinary vascular patterns. The combined output of both filters produces the final hand vascular patterns. Unlike the conventional hand vascular pattern extraction algorithm, the directional extraction approach prevents loss of the vascular pattern connectivity.

Person identification based on finger vein patterns is presented and evaluated using line tracking starting from different positions [6-7]. Local dark lines are identified and line tracking is executed by moving along the lines pixel by pixel. When a dark line is not detectable, a new tracking operation starts at another position. This iterative procedure detects the same line multiple times, so the line detection frequency is used to estimate the pixel vein probability.

An algorithm for finger vein pattern extraction in infrared images is proposed in [8]. The low contrast images, due to the light scattering effect, are enhanced and the fingerprint lines are removed using the *2D* discrete wavelet filtering. Kernel filtering produces multiple images by rotating the kernel in six different directions, focusing into the expected directions of the vein patterns. The maximum of all images is transformed into a binary image. Further improvement is achieved by a two-level morphological process: majority filter smoothes contours and removes some misclassified isolated pixels, and a reconstruction process removes the remaining misclassified regions. The final image is segmented into two regions, vein and tissue.

In [9], a certification system compares vein images for low-cost, high-speed, and high-precision vein extraction. The equipment for authentication consists of a near-infrared (*NIR*) light source and a monochrome *CCD* to produce contrast-enhanced images of the subcutaneous veins. In the recognition stage, phase correlation and template matching is applied. Several noise reduction filters, sharpness filters, and histogram manipulations are tested for best accuracy, giving in the overall system a high certification ratio.

Segmentation and vein thinning methods are studied in human hand infrared images and two new methods for threshold-based segmentation, based on endpoints, crossing points, and conditional thinning [10]. The distance-based matching experiments, used to detect vein patterns, show that this method is efficient for personal identification or verification purposes.

A method for localizing surface veins via *NIR* imaging and structured light ranging is presented in [11]. The eventual goal of the system is to serve as the guidance for a fully automatic catheterization device. The proposed system is based on *NIR* imaging, which has previously been shown effective in enhancing the visibility of surface veins. The vein regions in the *2D NIR* images are located using standard image processing techniques. A *NIR* line-generating *LED* module is used to implement structured light ranging and construct a *3D* topographic map of the arm surface. The located veins are mapped to the arm surface to provide a camera-registered representation of the arm and veins.

In [12-13], a Vein Contrast Enhancer (*VCE*) has been constructed to facilitate vein access by capturing an infrared image of veins, enhancing the contrast, and projecting the vein image back onto the skin in a typical displacement of 0.06 mm. Clinical evaluation of earlier monitor-based vein enhancement test systems has demonstrated the clinical utility of the infrared imaging technology used in the *VCE*.

In this paper, a novel method for finger vein segmentation in infrared images based on a model that represents the intensity distribution along a cross-sectional profile of vein, is proposed. The method is based on model fitting of brightness intensities over a local neighborhood. A simple second-order degree polynomial is used in order to represent the brightness intensities along the cross-sectional profile of veins. Two different approaches are adopted. According to the first, a multiscale multidirectional model fitting is performed based on the assumption that the second-order derivative on a vein pixel is positive. The second is based on multiscale model fitting of intensities in a single direction using two assumptions about the intensities of the profile of veins. According to the first assumption, the second-order derivative is positive on a vein pixel and according to the second, the first-order derivative is zero on a vein pixel which means that the pixel belongs to vein centerlines. The proposed method is robust, in both approaches, as the experimental results show and it achieves high evaluation rates in terms of sensitivity, specificity, and accuracy.

The remainder of this paper is organized as follows. In section 2, a detailed presentation of the proposed method for finger vein pattern extraction is given. In section 3, the experimental results are presented, and in section 4 the conclusions are given.

2. Proposed method

Fig. 1a shows an artificial finger vein image while Fig. 1b shows the distribution of intensities along a cross-sectional profile overlapped in the image of Fig. 1 (black line). As Fig.

*Corresponding Author: M. VLACHOS

1b shows, the distribution of intensities along a cross-sectional profile of the vein has a parabolic shape.

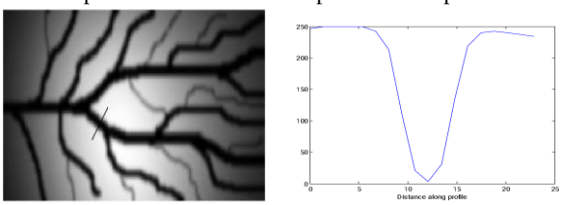

(a) (b)

Fig. 1. a. Artificial finger vein image, **b.** Distribution of intensities along a cross-sectional profile.

Thus, a simple second-order polynomial is used for fitting intensities over small local neighborhoods according to the well-known technique of sliding windows. The fitting is performed once for each desired scale and for every possible direction. The above procedure leads to an estimation problem of three unknown parameters (*a*, *b*, and *c*) for each pixel in every scale and direction.

To be more specific, a sliding window of size *(2w+1)x1*, where *2w+1* is the width of the cross-sectional profile (black line in fig. 1a), is applied in every pixel and a second-order polynomial (1) is used for fitting of the intensities of the pixels lie in the window:

$$y = f(x) = a \cdot x^2 + b \cdot x + c \quad (1)$$

, where *x* is the position of the pixel inside the sliding window (from *–w* to *w*), *y* is the corresponding intensity of brightness of the pixel located on *x* position and *a*, *b*, *c* are the parameters of the model to be estimated.

In the sequel, based on the assumption that a pixel belonging to the vein network has the minimum intensity along the cross-sectional profile, the minimum of (1) is computed. Differencing equation (1) with respect to *x* it yields:

$$\frac{dy}{dx} = 2 \cdot a \cdot x + b \quad (2)$$

On the other hand, the second-order derivative of (1) can be used for discrimination between concave and convex regions. The second-order derivative of (1) with respect to *x* shown in the following equation:

$$\frac{d^2 y}{dx^2} = 2 \cdot a \quad (3)$$

The fitting of the model inside the window leads to an over-defined system of equations, the solution of which gives the unknown parameters *a*, *b*, and *c*.

$$\begin{bmatrix} w^2 & -w & 1 \\ (1-w)^2 & (1-w) & 1 \\ (2-w)^2 & (2-w) & 1 \\ \bullet & \bullet & \bullet \\ \bullet & \bullet & \bullet \\ \bullet & \bullet & \bullet \\ 1 & -1 & 1 \\ 0 & 0 & 1 \\ 1 & 1 & 1 \\ \bullet & \bullet & \bullet \\ \bullet & \bullet & \bullet \\ \bullet & \bullet & \bullet \\ (w-2)^2 & (w-2) & 1 \\ (w-1)^2 & (w-1) & 1 \\ w^2 & w & 1 \end{bmatrix} \cdot \begin{bmatrix} a \\ b \\ c \end{bmatrix} = \begin{bmatrix} f(-w) \\ f(1-w) \\ f(2-w) \\ \bullet \\ \bullet \\ \bullet \\ f(-1) \\ f(0) \\ f(1) \\ \bullet \\ \bullet \\ \bullet \\ f(w-2) \\ f(w-1) \\ f(w) \end{bmatrix} \Rightarrow W \cdot u = f \quad (4)$$

, where *W* is the matrix of coefficients, *u* the vector of unknown parameters a, b, and c, and *f* the vector of intensities of the pixels lie in the window. Matrix *W* is invertible and thus the values of the unknown parameters can be estimated from the following formula:

$$u = W^{-1} \cdot f \quad (5)$$

By observing the first and second-order derivatives of equation (1) with respect to *x* the following assumptions can be made:

Assumption 1. A pixel belongs to vein network if $\frac{d^2 y}{dx^2} = 2 \cdot a > 0 \Rightarrow a > 0$.

Assumption 2. A pixel belongs to vein centerlines if $\frac{dy}{dx} = 2 \cdot a \cdot x + b = 0 \Rightarrow x = -\frac{b}{2 \cdot a}$.

Multiscale multidirectional model fitting.

The first approach is based only on the first assumption, i.e. detection of concave regions (positive second-order derivative) inside a window. A simple second-order degree polynomial is fitted for every scale along a cross-sectional profile of veins in four different directions (0, 45, 90, and 135 degrees). According to this approach, the estimation of the parameters of the model is performed for each pixel once for every scale *w* and for every possible direction *θ*. Thus, for every pixel multiple sets of parameters *a*, *b*, and *c* are derived:

$$u_{w\theta} = \begin{bmatrix} a_{w\theta} \\ b_{w\theta} \\ c_{w\theta} \end{bmatrix} = W^{-1} \cdot f_{w\theta} \quad (6)$$

, where $u_{w\theta}$ is the vector of unknown parameters *a*, *b*, and *c* at scale *w* and in the direction *θ*, $f_{w\theta}$ is the vector of intensities of pixels inside the window of size *wxw* pixels located in *θ* direction and *W* the vector of known coefficients.

A pixel belongs to vein network if at a specific direction *θ*, parameters $a_{w\theta}$ are positive for all scales. The final pattern is extracted using the logical *OR* of the pixels satisfying the above condition in all directions. In cases where a lot of

*Corresponding Author: M. VLACHOS

misclassifications are apparent on the binary image, a post-processing step is applied in order to remove the artifacts. This step includes a process known as length filtering.

Multiscale model fitting in a single direction.
The second approach is based on both assumptions. According to this vein, centerlines are detected by applying the procedure of estimation of the parameters of the model for each pixel once for every scale and in a single direction $\theta=0$. Thus, for every pixel multiple sets of parameters *a*, *b*, and *c* are derived:

$$u_{w0} = \begin{bmatrix} a_{w0} \\ b_{w0} \\ c_{w0} \end{bmatrix} = W^{-1} \cdot f_{w0} \quad . \qquad (7)$$

, where $u_{w\theta}$ is the vector of unknown parameters *a*, *b*, and *c* at scale *w* and in the horizontal direction ($\theta=0$), $f_{w\theta}$ is the vector of intensities of pixels inside the window of size *wxw* pixels located in horizontal direction, and *W* the vector of known coefficients.

A pixel belongs to vein network if at direction $\theta=0$ all the parameters a are positive (*Assumption 1:* $a_{w0} > 0$) and to vein centerlines if the value of *x* is near to zero (*Assumption 2*: $|x_{w0}| = \frac{b_{w0}}{2 \cdot a_{w0}} \le Tr$) for each scale, where *Tr* is a predefined threshold. Ideally, in order for a pixel to belong to vein centerlines the threshold *Tr*, according to the second assumption, should have zero value. In practice, due to noise presence and intensity inhomogeneities which are present both in real and artificial images, this condition is not satisfied. Consequently, the value of threshold *Tr* is estimated experimentally. The final pattern is extracted using the logical *OR* of the pixels satisfying the above condition. In cases where a lot of misclassifications are apparent on the binary image a post-processing step is applied in order to remove the artifacts. This step includes a process known as length filtering.

Length Filtering
In some images small misclassified isolated regions appear. These regions are removed from the binary image for more accurate finger vein pattern extraction by applying a process called length filtering. According to length filtering, the procedure of noise elimination is implemented as follows: A region of connected pixels is estimated from the binary image using the rule of eight-pixel connectivity. All regions with size less than a predefined threshold, experimentally derived, are eliminated. The remaining regions, surviving after length filtering, constitute the final vein pattern.

3. Experimental results

Image Acquisition. The original image is acquired using infrared illumination and an inexpensive monochrome *CCD* camera. The finger is located between the camera and a row of five infrared leds with adjustable illumination. Due to strong absorption of the hemoglobin in the near-infrared spectrum the veins are located in the dark areas of the image. Fig. 2 shows the experimental device used for image acquisition while fig. 3 shows an original infrared finger vein image and the corresponding region of interest (*ROI*) image extracted from it.

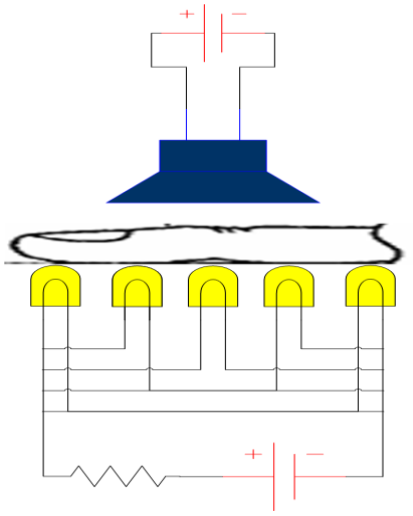

Fig. 2. Infrared image acquisition, experimental device.

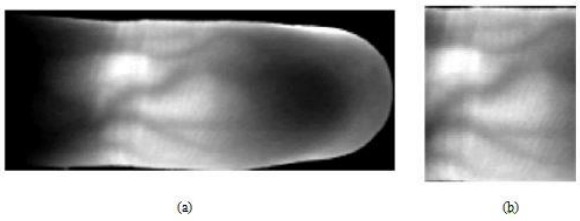

Fig. 3. a. Original infrared image **b.** *ROI* image.

Fig. 4 shows the results of the application of the proposed method (first approach) in the *ROI* image of fig. 3. b. Fig. 4. a. shows the *ROI* image while figures 4. b., c., d., e. show the binary images in four different directions (0, 45, 90, 135) and for seven different scales (*w*=3, 5, 7, 9, 11, 13, 15). These images are produced using the logical *AND* along scale for each direction. Finally, fig. 4. f. shows the extracted finger vein pattern which is the logical *OR* of the above four images along direction.

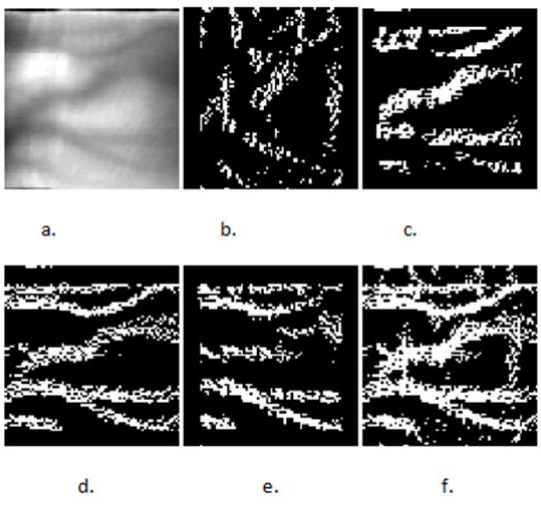

*Corresponding Author: M. VLACHOS

Fig. 4. a. *ROI* image, binary images **b.** θ=0, **c.** θ=45, **d.** θ=90, **e.** θ=135 for scales w=3, 5, 7, 9, 11, 13, 15 and **f.** logical *OR* of images b., c., d., e.

Fig. 5 shows the results of the application of the proposed method (second approach) on the *ROI* image of Fig. 3. b. Fig. 5. a. shows the *ROI* image while figures 5. b., c., d., e., f., g., h. show the binary images in seven different scales (w=3, 5, 7, 9, 11, 13, 15) at a single (horizontal) direction (θ=0). These images are produced using a threshold value Tr=1. The selection of an appropriate value for the parameter Tr is a compromise between robust detection of the finger vein network and presence of artifacts in the final segmentation result. A larger value for this parameter produces a larger number of misclassified pixels. On the other hand, a selection of a small value for this parameter may result in a loss of a part of the finger vein network. Finally, fig. 5. i. shows the extracted finger vein pattern which is the logical *OR* of the above seven images along scale.

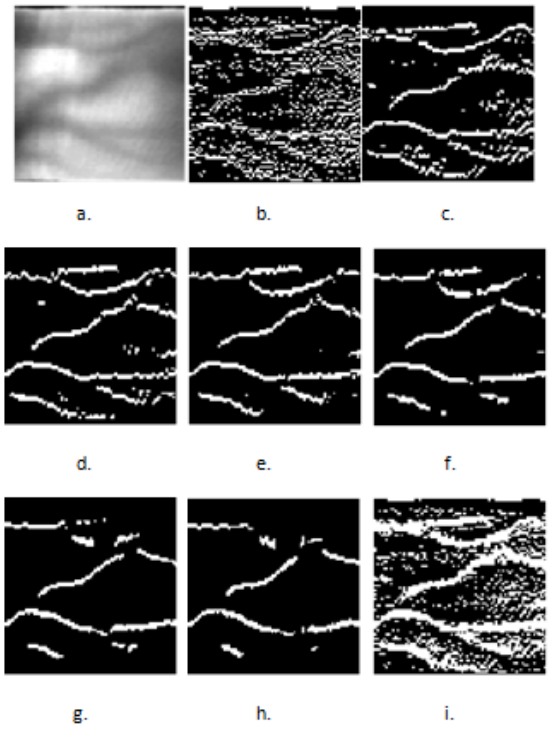

Fig. 5. a. *ROI* image, binary images **b.** w=3, **c.** w=5, **d.** w=7, **e.** w=9, **f.** w=11, **g.** w=13, **h.** w=15 for horizontal direction θ=0 and **i.** logical *OR* of images b., c., d., e., f., g., h.

Artificial image database. A quantitative evaluation of the proposed method in real infrared images is difficult due to the absence of manual segmentation data. The extremely low contrast images increase the disagreement of human annotation. Therefore, the proposed method is evaluated using a small set of images, each one created by the weighted sum of the two artificial images. The first image is constructed using an artificial vein-like network. This network consists of connected lines of different widths with junctions and bifurcations and multiple low pass filtering to simulate the blurriness of the edges which is apparent to the real images due to the blood flow and scattering effects. The second artificial image is used to simulate the nonuniform image background of real infrared images which is created by applying an iterative spatial low pass Gaussian filter with a large window size to the original infrared image.

Evaluation rates. In the finger vein segmentation process, each pixel is classified as tissue (non-vein) or vein. Consequently, there are four events, true positive (*TP*) and true negative (*TN*) when a pixel is correctly segmented as vein or non-vein, and two misclassifications, a false negative *(FN)* appears when a pixel in a vein is segmented in the non-vein area, and a false positive (*FP*) when a non-vein pixel is segmented as a vein pixel.

Two widely known statistical measures are used for method evaluation: sensitivity and specificity, which are used to evaluate the performance of the binary segmentation outcome. The sensitivity is a normalized measure of true positives, while specificity measures the proportion of true negatives:

$$sensitivity = \frac{TP}{TP + FN}, \quad (8)$$

$$specificity = \frac{TN}{TN + FP}. \quad (9)$$

Usually, there is a tradeoff between two measures. Finally, the accuracy of the binary classification is defined by:

$$accuracy = \frac{TP + TN}{P + N}, \quad (10)$$

where P and N represent the total number of positives (vein) and negatives (non-vein) pixels in the segmentation process and is the degree of conformity of the estimated binary classification to the true according to a manual segmentation. Thus, the accuracy is strongly related to the segmentation quality and for this reason, is used to evaluate and compare different methods.

The proposed method is evaluated on the artificial image database. Each image of the set is constructed according to the above procedure.

Table 1 shows the mean sensitivity, specificity, and accuracy of the proposed method on the artificial finger image database with the approach of multiscale multidirectional model fitting without post-processing while table 2 shows the same rates for the same approach with post-processing.

Fig. 6 shows the first image of the artificial finger database and the corresponding vein network obtained by the application of the proposed method and the approach of multiscale multidirectional model fitting without post-processing. Fig. 7 shows the first image of the artificial finger database and the corresponding vein network obtained by the application of the proposed method and the approach of multiscale multidirectional model fitting with post-processing.

Table 3 shows the mean sensitivity, specificity, and accuracy of the proposed method on the artificial finger image database with the approach of multiscale model fitting on a single direction without post-processing while table 4 shows the same rates for the same approach with post-processing.

Fig. 8 shows the first image of the artificial finger database and the corresponding vein network obtained by the

*Corresponding Author: M. VLACHOS

application of the proposed method and the approach of multiscale model fitting on a single direction without post-processing. Fig. 9 shows the first image of the artificial finger database and the corresponding vein network obtained by the application of the proposed method and the approach of multiscale model fitting on a single direction with post-processing.

Table 1. Mean sensitivity, specificity, and accuracy of the proposed method (first approach) without post-processing.

	Sensitivity	***Specificity***	***Accuracy***
Mean	0.945	0.929	0.933
Standard Deviation	0.117	0.033	0.049

Table 2. Mean sensitivity, specificity, and accuracy of the proposed method (first approach) with post-processing.

	Sensitivity	***Specificity***	***Accuracy***
Mean	0.926	0.963	0.956
Standard Deviation	0.115	0.027	0.045

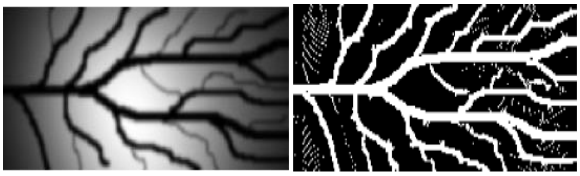

Fig. 6. The first image of the artificial finger image database and the corresponding finger vein pattern obtained by the application of the proposed method (first approach) without post-processing.

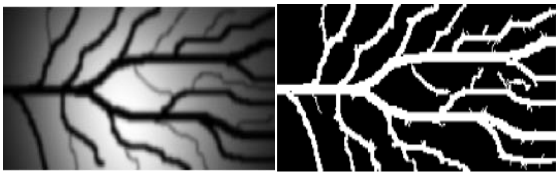

Fig. 7. The first image of the artificial finger image database and the corresponding finger vein pattern obtained by the application of the proposed method (first approach) with post-processing.

Table 3. Mean sensitivity, specificity, and accuracy of the proposed method (second approach) without post-processing.

	Sensitivity	***Specificity***	***Accuracy***
Mean	0.876	0.853	0.858
Standard Deviation	0.092	0.031	0.043

Table 4. Mean sensitivity, specificity, and accuracy of the proposed method (second approach) with post-processing.

	Sensitivity	***Specificity***	***Accuracy***
Mean	0.841	0.919	0.901
Standard Deviation	0.090	0.041	0.046

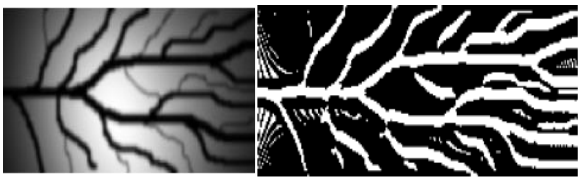

Fig. 8. The first image of the artificial finger image database and the corresponding finger vein pattern obtained by the application of the proposed method (second approach) without post-processing.

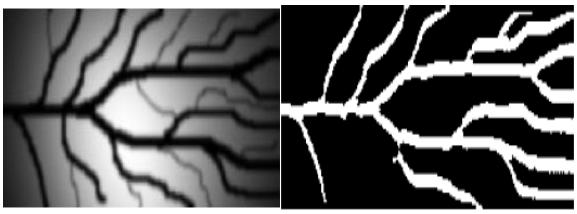

Fig. 9. The first image of the artificial finger image database and the corresponding finger vein pattern obtained by the application of the proposed method (second approach) with post-processing.

From the results shown on tables 1-4 and in the figures 6-9 arises that the proposed method is robust. Moreover, the first approach achieves higher evaluation rates than the second.

4. Conclusions

In this paper, a novel method for finger vein segmentation in infrared images based on a model that represents the intensity distribution along a cross-sectional profile of vein, is proposed. The method is based on model fitting of brightness intensities over a local neighborhood. A simple second-order degree polynomial is used in order to represent the brightness intensities across the cross-sectional profile of veins. Two different approaches are adopted. According to the first, a multiscale multidirectional model fitting is performed based on the assumption that on a vein pixel the second-order derivative is positive. The second is based on multiscale model fitting of intensities in a single direction using two assumptions about the intensities of the profile of veins. According to the first, the second order derivative is positive on a vein pixel, and to the second, the first order derivative is zero on a vein pixel which means that the pixel belongs to vein centerlines. The proposed method is robust, in both approaches, as the experimental results show and it achieves high evaluation rates in terms of sensitivity, specificity, and accuracy. In addition, it can be applied in various image processing problems which require segmentation of tubular structures in digital images such as segmentation of vessels in retinal images, leaf vein extraction, and road extraction from satellite images.

5. Acknowledgments

This work is partially supported by grant

*Corresponding Author: M. VLACHOS

KARATHEODORIS of the University of Patras.

6. References

1. G.T. Park, S.K. Im, and H.S. Choi, "A Person Identification Algorithm Utilizing Hand Vein Pattern", Proc. of Korea Signal Processing Conf., Vol. 10, No. 1, 1997, pp. 1107-1110.
2. D.U. Hong, S.K. Im, and H.S. Choi, "Implementation of Real-Time System for Personal Identification Algorithm Utilizing Hand Vein Pattern", Proc. of IEEK Fall Conf., 1999, Vol. 22, No. 2, pp. 560-563.
3. S.K. Im, H.M. Park, S.W. Kim, C.K. Chung, and H.S. Choi, "Improved Vein Pattern Extracting Algorithm and its Implementation", Proc. of IEEE ICCE, 2000, pp. 2-3.
4. S.K. Im, H.M. Park, and S.W. Kim, "A Biometric Identification System by Extracting Hand Vein Patterns", Journal of the Korean Physical Society, Vol. 38, No. 3, 2001, pp. 268-272.
5. S.K. Im, H.S. Choi, and S.W. Kim, "Direction-Based Vascular Pattern Extraction Algorithm for Hand Vascular Pattern Verification", Korea University, Seoul, Korea. ETRI Journal, Vol. 25, No. 2, April 2003.
6. N. Miura, A. Nagasaka, T. Miyatake, "Feature extraction of finger-vein patterns based on repeated line tracking and its application to personal identification", Machine Vision and Applications (2004) Vol. 15, pp.194-203.
7. N. Miura, A. Nagasaka, T. Miyatake, "Feature extraction of finger-vein patterns based on iterative line tracking and its application to personal identification", Systems and Computers in Japan, Vol. 35, No. 7, 2004.
8. M. Vlachos, and E. Dermatas, "A finger vein pattern extraction algorithm based on filtering in multiple directions", 5th European Symposium on Biomedical Engineering, July 2006.
9. T. Tanaka, N. Kubo, "Biometric Authentication by Hand Vein Patterns", SICE Annual Conference in Sapporo, August 2004.
10. Y. Ding, D. Zhuang, and K. Wang, "A Study of Hand Vein Recognition Method", Proceedings of the IEEE International Conference on Mechatronics & Automation, Niagara Falls, Canada, July 2005.
11. V. Paquit, J.R. Price, R. Seulin, F. Meriaudeau, R.H. Farahi, K.W. Tobin and T.L. Ferrell, "Near-infrared imaging and structured light ranging for automatic catheter insertion".
12. H.D. Zeman, G. Lovhoiden, and C. Vrancken, "The Clinical Evaluation of Vein Contrast Enhancement", Proc. SPIE, vol. 4615, pp.61-70, 2002.
13. H.D. Zeman, G. Lovhoiden, and C. Vrancken, "Prototype Vein Contrast Enhancer", Proc. SPIE, vol. 5318, in press, 2004.
14. C.H. Wu, G. Agam, P. Stanchev, "A general framework for vessel segmentation in retinal images", International Symposium on Computational Intelligence in Robotics and Automation (CIRA), June 2007 pp. 37 – 42.

*Corresponding Author: M. VLACHOS